Crowding-induced structural alterations of random-loop chromosome model

Jun Soo Kim

Department of Biomedical Engineering and Chemistry of Life Processes Institute, Northwestern University, Evanston, IL 60208, USA and

Department of Chemistry and Nano Science, Ewha Womans University, Seoul 120-750, Korea

Vadim Backman and Igal Szleifer*

Department of Biomedical Engineering and Chemistry of Life Processes Institute, Northwestern University, Evanston, IL 60208, USA

(Received March 14, 2011)

Abstract

We investigate structural alterations of random-loop polymers due to changes in crowding condition, as a model to study environmental effects on the structure of chromosome subcompartments. The polymer structure is changed in a non-monotonic fashion with increasing density of crowders: condensed at small volume fractions; decondensed at high crowding volume fractions. The non-monotonic behavior is a manifestation of the non-trivial distance dependence of the depletion interactions. We also show that crowding-induced structural alterations affect the access of binding proteins to the surface of polymer segments and are distinguished from structural changes due to the increased number of specific polymer loops.

PACS numbers: 82.35.Lr, 87.16.A-, 87.16.Sr, 87.17.Aa

A cell is crowded with a high content of macromolecules occupying up to 40 % of the total volume [1], and crowding effects on nuclear structures and functions have been of great interest in recent years [2–5]. Especially, since the eukaryotic chromosome structure affects genome functions, such as transcription, DNA replication and repair, and repression of gene expression [6], understanding of the chromosome structure in the crowded environment is critical to further our understanding of genomic events in cell nuclei. Furthermore, crowding conditions may be altered significantly, for instance, by acute changes in cell volume which may occur due to changes in osmolarity under normal and pathological conditions [7]. Therefore, there has been considerable interest in understanding the effects of changes in the crowding condition on the chromosome structure [4, 5].

In this work we investigate structural alterations of chromosome domains called subcompartments [6, 8], induced by changes in the volume fraction occupied by crowding macromolecules (ϕ_c). Several models of a chromosome have been proposed that can reproduce currently available experimental data such as fluorescence *in situ* hybridization (FISH) [9, 10] and chromosome conformation capture (3C) and other 3C-based techniques [11–13]: the random-walk/giant-loop model [9], the multiloop subcompartment model [8], the random loop model [14], and the decondensing linear polymer model [15] for the mean square intrachromosome distances measured with FISH experiments; the crumpled globule model [16**?**] for the contact probabilities with 3C-based techniques; and the kinkable chromatin fiber model [17] for both properties. In this work, a random-loop (RL) polymer is employed to model a chromosome subcompartment, containing DNA contents of about 1 Mbp, since we believe that the RL polymer can reasonably describe the presence of a chromosome subcompartment by assuming chromatin loops of different lengths. We verify that the conclusions of this work are true for all polymers and do not depend on a specific chromosome model, by studying the role of crowding on self-avoiding walk (SAW) polymers. Crowding effects are investigated by applying depletion potentials determined at different ϕ_c to polymer segments. In this work we focus on the crowding effects induced by excluded volume interactions between particles. Interestingly, it is found that the crowding-induced structural alterations of RL polymers are non-monotonic with increasing ϕ_c. We also show that the crowding-induced structural changes have different biological implications from those induced by the increased number of polymer loops, resulting in different accessibility of binding proteins to the surface of RL polymers.

An RL polymer is a linear polymer whose segments pair with each other via harmonic potential according to a looping probability p_{lp} [14]. For each polymer consisting of 300 segments we consider three looping probabilities, $p_{lp} = 3 \times 10^{-4}$, 6×10^{-4}, and 9×10^{-4}, according to which 13, 25, and 37 pairs of segments are looped, forming more compact RL polymers in order. These looping probabilities are chosen such that volume fractions of the center of a RL polymer cover a range of 0.15, 0.23, and 0.29 respectively, comparable to the chromatin volume fractions between 0.1 and 0.4 in biological cells. A diameter (d_s) of each polymer segment is set to 5σ (= 30 nm) assuming the formation of a chromatin fiber with a thickness of 30 nm, where σ is the unit of length and is the diameter of crowding macromolecules included implicitly via depletion potentials. The 30 nm fibers have been observed *in vitro* at physiological salt concentrations and is assumed in this model although there is a lack of *in vivo* evidence [18]. Cellular environments are polydisperse media consisting of macromolecules with various sizes. The size of crowding macromolecules is fixed in this work, to capture the main role that complex depletion interactions have on the macromolecules, and we defer the consideration of polydispersity effects to future work. The average molecular weight of the proteins distributed in the nucleoplasm is 67.7 kDa [19], corresponding to a diameter of about 6 nm assuming a spherical shape of proteins and a partial specific volume of 0.73 ml/g. This explains the choice of $\sigma = 6$ nm. Representative conformations of RL

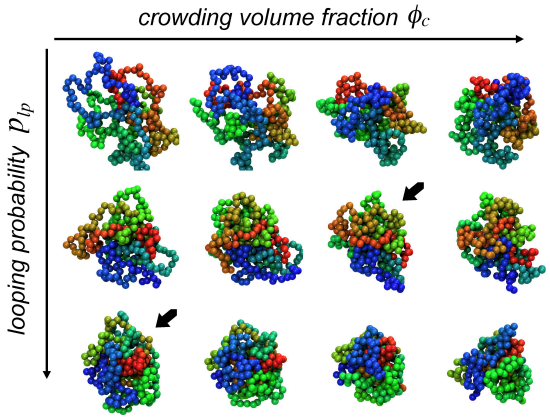

FIG. 1: Representative configurations of RL polymers with $p_{lp} = 3 \times 10^{-4}$, 6×10^{-4}, and 9×10^{-4} (each from top to bottom) and with $\phi_c = 0.0$, 0.1, 0.2, and 0.3 (each from left to right). Color varies for polymer segments from red, to green, and to blue. See text below Figure 4 for black arrows.

polymers are shown in Figure 1. The structure of RL polymers is altered either by changing p_{lp}, thus the number of polymer loops, or by changing ϕ_c. RL polymers are condensed with increasing numbers of polymer loops. The structural alterations of RL polymers due to changes in ϕ_c are discussed throughout this letter.

Each segment in a RL polymer is assumed to interact with other segments by a modified repulsive Lennard-Jones (LJ) potential $U_r(R) = 4\epsilon\left[(\sigma/(R-r_0))^{12} - (\sigma/(R-r_0))^6\right] + \epsilon$ for $r_0 < R < r_0 + r_c$ and 0 elsewhere, where ϵ is a LJ well-depth and set to k_BT, R is a center-to-center distance between polymer segments, $r_0 = 4\sigma$, and $r_c = 2^{1/6}\sigma$. Bonded segments interact with a combination of the repulsive LJ potential described above and the finite extension nonlinear elastic (FENE) potential $U_b(R) = -\frac{1}{2}k_bR_b^2\ ln\ \left[1-((R-r_0)/R_b)^2\right]$, where $r_0 = 4\sigma$, $k_b = 30k_BT/\sigma^2$, and $R_b = 1.5\sigma$. The RL polymers are first equilibrated with molecular dynamics simulations for a simulation duration of one million time steps, which is more than ten times longer than the autocorrelation time of the radius of gyration. The polymers are further equilibrated using Brownian dynamics (BD) simulations for another one million time steps [20]. Hydrodynamic interactions are not considered in BD simulations. A time step $\Delta t = 10^{-4}\tau_{BD}$ is used for BD simulations, where τ_{BD} is the time for a polymer segment to move a distance of σ with diffusion coefficient D ($\tau_{BD} = \sigma^2/D$). It is verified that the polymer segments move an average distance of 0.02σ (=0.12 nm) for the given time step, which is small enough to prevent polymer segments from jumping unphysically large distances. All simulations are performed with GROMACS version 4.0.5 [21]. Statistical properties of RL polymers are calculated from a total of 150,000 independent polymer configurations for a given p_{lp}. Independent configurations are prepared following Ref. [14], that is, by simulations of 500 different sets of looping pairs for a given p_{lp} and 300 independent initial configurations for each set of looping pairs.

Simulations of RL polymers in the explicit presence of crowding macromolecules would be prohibitively long to obtain statistical properties. Instead, the effect of crowding macromolecules is included implicitly by applying to polymer segments the depletion potentials determined in the explicit presence of crowding macromolecules, as shown in Figure 2. A range of ϕ_c between 0.0 and 0.3 is studied. The depletion potentials have been obtained from constraint-biased molecular dynamics simulations of short polymers in the presence of crowding macromolecules in previous work [22]. We also have shown that the implicit simulations of a polymer with depletion potentials result in the polymer properties in a rea-

sonable agreement with those obtained from explicit simulations in the presence of crowding macromolecules [22]. Thus, we expect the depletion potential to be a very good representation of the explicit crowders. Therefore, we simulate the polymers with the addition of the depletion potentials shown in Fig. 2 to represent the crowding agents.

The potentials in Figure 2 show two main effects induced by crowding macromolecules. For non-zero ϕ_c, attractive minima can be found at short distances and they become deeper with increasing ϕ_c. The repulsive barrier becomes more pronounced as well when ϕ_c increases. The effective attraction can be explained in terms of entropy gain of the crowding macromolecules, or unbalanced osmotic pressure exerted by the macromolecules when polymer segments approach each other. Repulsive barriers, however, are induced due to presence of the crowding macromolecules within a gap between polymer segments. When the separation between polymer segments is large enough for crowding molecules to be arranged between the polymer segments, the polymer segments need to squeeze out the crowding molecules in order to approach each other (for details see Ref. [22]).

Interestingly, structural alterations of RL polymers are non-monotonic with increasing ϕ_c when the depletion potentials in Figure 2 are applied to RL polymer segments. The RL polymers are condensed with increase of crowding at small ϕ_c, while they become decondensed with further increase of crowding at higher ϕ_c, see also Fig. 1. Such structural alterations are presented in terms of the size of RL polymers in Figure 3 (a). The size of RL polymers, defined as the radius of gyration ($\langle R_g^2 \rangle^{1/2}$), varies in a non-monotonic fashion with changes in ϕ_c: decreases with crowding from $\phi_c = 0.0$ to 0.2; then increases from $\phi_c = 0.2$ to 0.3. To show the generality of our results, i.e. that the non-monotonic behavior is not a result of the particular model chosen for the chromosomes, we studied the role of the depletion

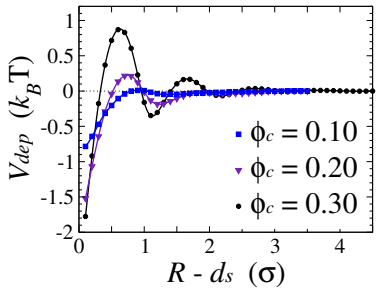

FIG. 2: Depletion potential, V_{dep}, as a function of $(R - d_s)$ where R is a center-to-center distance between polymer segments and d_s is the diameter of the segments, 5σ.

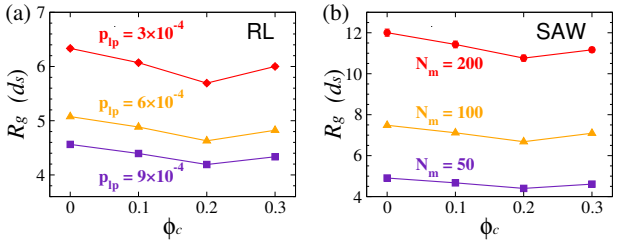

FIG. 3: Radius of gyration of (a) RL polymers (for different p_{lp}) and (b) SAW polymers (for different polymer lengths, N_m) as a function of ϕ_c. Error estimates are less than the size of symbols, and solid lines are included as guides to the eye.

potentials on SAW polymers (equivalent to a RL polymer with $p_{lp} = 0.0$) with the number of monomers $N_m = 50$, 100, and 200. As shown in Figure 3 (b), the non-monotonic effect is clearly observed. These results indicates that the non-monotonic structural alterations by crowding are a generic effect that arises from the depletion potential induced by the presence of crowding agents smaller than the polymer segments.

Osmotic stress has been applied to increase macromolecular crowding in the cell nucleus [4, 5]. Hyper-condensation of chromatin, identified by chromatin clumping, was observed with increased osmolarity and, equivalently, with increased crowding [4, 5]. The hyper-condensation of chromatin, however, does not simply continue to increase with osmolarity. Further increase of hyper-condensation was not observed at the highest osmolarities in Ref. [4], and hyper-condensation rather seems to decrease at the highest osmolarities, see Fig. 1 in Ref. [5] . These experimental observations partially support the non-monotonic crowding effects on the structure of RL polymers. However, more quantitative measurements are required to firmly confirm our conclusions.

It may seem counterintuitive that the crowding effects on the structure of RL polymers are reversed (decondensed) with increase of ϕ_c between 0.2 and 0.3. The polymer condensation with increasing ϕ_c between 0.0 and 0.2 can be understood by stronger attractive forces between polymer segments due to crowding, as depicted by depletion potentials in Figure 2. The polymer decondensation going from $\phi_c = 0.2$ to 0.3, however, is not obvious since attractive forces still increase with ϕ_c. However, a close look at the depletion potentials, Figure 2, reveals that the repulsive barrier also increases with increasing ϕ_c, and the difference between the repulsive maximum and the attractive minimum increases with ϕ_c, amounting to $1.5k_BT$ and $2.7k_BT$ at ϕ_c=0.2 and 0.3, respectively. The connectivity of the

polymer segments implies that if the molecules maximize the number of neighbors at the distance corresponding to the potential minimum, there is a very large number of segments that are found at a distance corresponding to maximal repulsion. The optimization of maximizing the number of segments at the potential minimum while minimizing the number at the potential maximum results in the non-monotonic behavior and it demonstrates that this effect is independent of the polymer model, but it is rather the effect induced by the presence of high concentrations of crowding agents smaller than the polymer segments.

Crowding-induced structural alterations predicted for RL polymers have important biological implications in the access of nuclear proteins to the surface of chromatin fibers, which is the key step to initiate a variety of genomic processes [23, 24]. Accessibility of nuclear proteins is investigated by calculating the accessible surface area of RL polymers in different crowding conditions. We assume a spherical probe with diameter d_p, and then the excluded volume to the probe is defined by a spherical volume of radius $(d_s + d_p)/2$ centered at each polymer segments. The surface of the excluded volume is defined as the accessible surface to the probe. Total accessible surface area (ASA) is calculated numerically [25] for a probe of $d_p = 2\sigma = 12$ nm, a typical size for a transcription factor, and the ASA normalized by that of $p_{lp} = 3 \times 10^{-4}$ at $\phi_c = 0.0$ is presented in Figure 4.

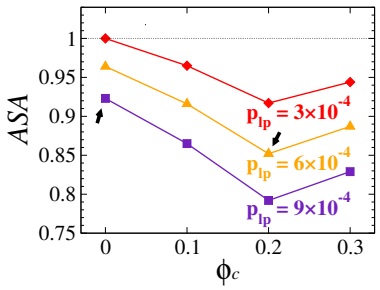

FIG. 4: Normalized ASA. Black arrows point to two cases where the sizes and densities of polymers are similar but the ASA's are different (see text).

The ASA depends on ϕ_c in a non-monotonic fashion as the chromosome size does. From $\phi_c = 0.0$ to 0.2 the ASA decreases by 10∼15 % for the three p_{lp}. It was shown that large macromolecules including the transcription factor TFIIH can readily access the interior of condensed chromatin domains [24]. We have verified that the ASA changes even more in the dense polymer core, with up to 30% decrease of ASA. This study suggests that crowding-induced structural alterations of chromosomes may have a crucial impact on the

accessibility of DNA-binding proteins and thus the kinetics of genome functions including gene transcription.

Finally, the structural alterations induced by crowding are compared with those induced by increased number of specific polymer loops. We specifically consider the structure of RL polymers at $p_{lp} = 6 \times 10^{-4}$ and $\phi_c = 0.0$. The polymers can be condensed by increasing either p_{lp} or ϕ_c. In Figure 3, the size of condensed polymers are almost the same when p_{lp} is increased to 9×10^{-4} with fixed ϕ_c as when ϕ_c is increased to 0.2 with fixed p_{lp} (also see black arrows in Figure 1). Interestingly, the ASA's calculated in these two cases (marked with black arrows in Figure 4) are significantly distinct in spite of similar polymer size. This suggests that the internal structure of a condensed polymer by non-specific depletion interactions can be quite different from that induced by increase of specific polymer loops.

It is important to note that this work focuses on crowding effects due to the excluded volume interactions of monodisperse depleting spheres. The strength and range of depletion potentials depend on the sizes of polymer segments and depleting spheres as well as on the interactions between these particles. Biological environments including the cell nucleus are, indeed, polydisperse media with macromolecules of varying molecular weights, and the macromolecules therein interact with each other via nonspecific interactions such as electrostatic and van der Waals interactions in addition to the excluded volume interactions. Therefore, the study of crowding effects due to the presence of polydisperse depleting spheres interacting via other nonspecific interactions represents possible future directions of this work. The present work however, presents a novel effect that will be present in all environments due to the fact that excluded volume interactions are ubiquitous in all molecular systems.

In summary, the structure of random-loop (RL) polymers modeling chromosome subcompartments is altered in a non-monotonic fashion by the crowding effects induced by a high content of macromolecules in the cell nucleus. RL polymers are condensed with crowding at small ϕ_c, whereas they become decondensed with further crowding at higher ϕ_c. The non-monotonic behavior with increasing crowding results from a balance between maximizing the number of close neighbors while minimizing the number of segments at distances corresponding to maximal depletion repulsions. Although this work is performed with a specific model of chromosome subcompartments, the crowding-induced structural alterations predicted here are a generic effect arising from a balance between these two competing effects

arising from the depletion interactions. Therefore, changes in the crowding condition of cellular environments may have a significant influence in the kinetics of genomic activities, as shown by changes in the accessibility of binding proteins to the surface of polymer segments. It is also found that polymer size is not enough to characterize the properties of the model chromosomes, the polymer structure altered by non-specific crowding effect is distinct from that altered by specific polymer looping.

This work is supported by the National Science Foundation under grant EFRI CBET-0937987.

* Electronic address: igalsz@northwestern.edu

[1] R. J. Ellis and A. P. Minton, Nature **425**, 27 (2003).

[2] S. B. Zimmerman, Biochim. Biophys. Acta **1216**, 175 (1993).

[3] R. Hancock, J. Struct. Biol. **146**, 281 (2004).

[4] H. Albiez *et al.*, Chromosome Res. **14**, 707 (2006).

[5] K. Richter, M. Nessling, and P. Lichter, J. Cell Sci. **120**, 1673 (2007).

[6] N. Naumova and J. Dekker, J. Cell Sci. **123**, 1979 (2010).

[7] F. Lang *et al.*, Physiol. Rev. **78**, 247 (1998).

[8] C. Münkel *et al.*, J. Mol. Biol. **285**, 1053 (1999).

[9] R. K. Sachs *et al.*, Proc. Natl. Acad. Sci. USA **92**, 2710 (1995).

[10] T. Cremer and C. Cremer, Nat. Rev. Genet. **2**, 292 (2001).

[11] J. Dekker *et al.*, Science **295**, 1306 (2002).

[12] E. Lieberman-Aiden *et al.*, Science **326**, 289 (2009).

[13] Z. Duan *et al.*, Nature **465**, 363 (2010).

[14] J. Mateos-Langerak *et al.*, Proc. Natl. Acad. Sci. USA **106**, 3812 (2009).

[15] A. Rosa and R. Everaers, PLoS Comput. Biol. **4**, e1000153 (2008).

[16] A. Grosberg *et al.*, Europhys. Lett **23**, 373 (1993).

[17] A. Rosa, N. B. Becker, R. Everaers, Biophys. J. **98**, 2410 (2010).

[18] D. J. Tremethick, Cell **128**, 651 (2007).

[19] W. A. Bickmore and H. G. E. Sutherland, EMBO J. **21**, 1248 (2002).

[20] D. L. Ermak and J. A. McCammon, J. Chem. Phys. **69**, 1352 (1978).

[21] D. van der Spoel *et al.*, J. Comput. Chem. **26**, 1701 (2005).

[22] J. S. Kim and I. Szleifer, J. Phys. Chem. C **114**, 20864 (2010).

[23] M. Beato and K. Eisfeld, Nucleic Acids Res. **25**, 3559 (1997).

[24] P. J. Verschure *et al.*, EMBO Rep. **4**, 861 (2003).

[25] T. Ooi *et al.*, Proc. Natl. Acad. Sci. USA **84**, 3086 (1987).

Figure Captions

Figure 1.

Representative configurations of RL polymers with $p_{lp} = 3 \times 10^{-4}$, 6×10^{-4}, and 9×10^{-4} (each from top to bottom) and with ϕ_c = 0.0, 0.1, 0.2, and 0.3 (each from left to right). Color varies for polymer segments from red, to green, and to blue. See text below Figure 4 for black arrows.

Figure 2.

Depletion potential, V_{dep}, as a function of $(R - d_s)$ where R is a center-to-center distance between polymer segments and d_s is the diameter of the segments, 5σ.

Figure 3.

Radius of gyration of (a) RL polymers (for different p_{lp}) and (b) SAW polymers (for different polymer lengths, N_m) as a function of ϕ_c. Error estimates are less than the size of symbols, and solid lines are included as guides to the eye.

Figure 4.

Normalized ASA. Black arrows point to two cases where the sizes and densities of polymers are similar but the ASA's are different (see text).